

THE PULSED RF SUPERCONDUCTIVITY PROGRAM AT SLAC*

ISIDORO E. CAMPISI AND Z. DAVID FARKAS
*Stanford Linear Accelerator Center
Stanford University, Stanford, California 94305*

Abstract

Recent tests performed at SLAC on superconducting TM_{010} cavities using short rf pulses ($\leq 2.5\mu s$) have established that at the cavity surface magnetic fields can be reached in the vicinity of the theoretical critical fields without an appreciable increase in average losses. Tests on niobium and lead cavities are reported.

The pulse method seems to be best suited to study peak field properties of superconductors in the microwave band, without the limitations imposed by defects. The short pulses also seem to be more effective in decreasing the causes of field emission by rf processing.

Applications of the pulsed rf superconductivity to high-gradient linear accelerators are also possible.

* Work supported by the Department of Energy, contract DE-AC03-76SF00515

1. Introduction

Over the past couple of years tests have been performed at SLAC using part of the power provided by a 36 MW, 2856 MHz, 2.5 μ s pulse length klystron. Originally the klystron was used for peak-field, room-temperature, rf processing on a Nb cavity which was being tested for cw field breakdown. It was realized that, when operated in the short pulse mode, the superconducting Nb cavity could withstand fields considerably higher than in cw without appreciable losses. This fact has led us to extend the tests on several cavities, in the belief that this method has the potential both for studies of fundamental properties of superconductors under the action of rf fields at a frequency that traditionally has not provided good experimental information, and also for some special accelerator application, typically in high-gradient, pulsed, linear electron accelerators.

Other investigators had previously tested superconducting cavities with pulses as short as several tens of microseconds or longer,^{1,2,3} but no systematic experimental study of the properties of superconductors had ever been carried out before in the microwave band with short pulses. Part of the reason lies in the fact that very few laboratories are equipped with the short-pulse, high peak-power microwave sources necessary to perform this type of investigation. From this point of view, SLAC is singularly well equipped for this type of tests, the only limitations being that the longest pulse length available is about 2.5 μ s and that all of the tests are done at a frequency of about 2856 MHz.

The tests have been so far performed on TM_{010} cavities, but preparations are under way to study the properties of superconductors with one or more TE_{011} cavities. This approach should provide information about the superconductors without interference from field-emitted electrons and bremsstrahlung x-rays. So far results for niobium and lead have been obtained, while work is in progress to test the properties of Nb_3Sn and tin.

2. Theory of the Pulsed Mode Operation

The details of the calculations used to describe the behavior of a cavity operated in the pulsed mode have been given elsewhere.^{4,5,6} In this type of operation it is necessary to choose the external Q of the cavity in such a way that the maximum

possible amount of energy in the incident pulse can be transferred to the cavity. The optimum transfer efficiency, in the case in which $Q_0 \gg Q_e$, is obtained for

$$Q_e = 2.5 f T_p \quad (1)$$

where Q_e is the external quality factor of the cavity, f is the frequency of the rf and T_p is the pulse length. For a pulse length of $2.5 \mu\text{s}$ at $f \sim 2856 \text{ MHz}$, the maximum transfer is achieved for $Q_e \simeq 18,000$. Figure 1 shows the reflected and emitted power curves for a $T_p = 2.5 \mu\text{s}$ and various values of the cavity's Q_e . Figure 2 gives the transfer efficiency as a function of the external Q , for the two pulse lengths of 1.0 and $2.5 \mu\text{s}$. The maximum possible transfer efficiency is about 80%.

Unlike in the case of long pulse or cw operation, for which the measurement of the energy stored in the cavity (and, consequently, of the fields in it) can be done by determining the coupling coefficient and the incident cw power, the measurement of the fields in a cavity operated in the pulsed mode requires the determination of peak, transient-like properties. Typically, though, transient measurements have low accuracy and the agreement between measurements performed on different pulses is not very good.

Instead, we determine the peak fields in the cavity using an average power method which is very accurate for strongly-coupled cavities with low losses. Under the latter condition, the decay of the power past the end of the incident power pulse (emitted power) is dominated by the external Q , while the losses have a negligible contribution. If one can integrate the power curve, then, in the low-loss condition, one can obtain the energy stored in the cavity at the end of the charging pulse:

$$U_s = \int_{T_p}^{\infty} P_e(t) dt \quad (2)$$

In the case in which the losses are non-negligible, Eq. (2) still represents a lower limit to the energy stored in the cavity.

Once the stored energy is known, the peak surface fields in the cavity can be determined as

$$E_s = k \sqrt{U_s} \quad (3)$$

$$H_s = k' \sqrt{U_s} \quad (4)$$

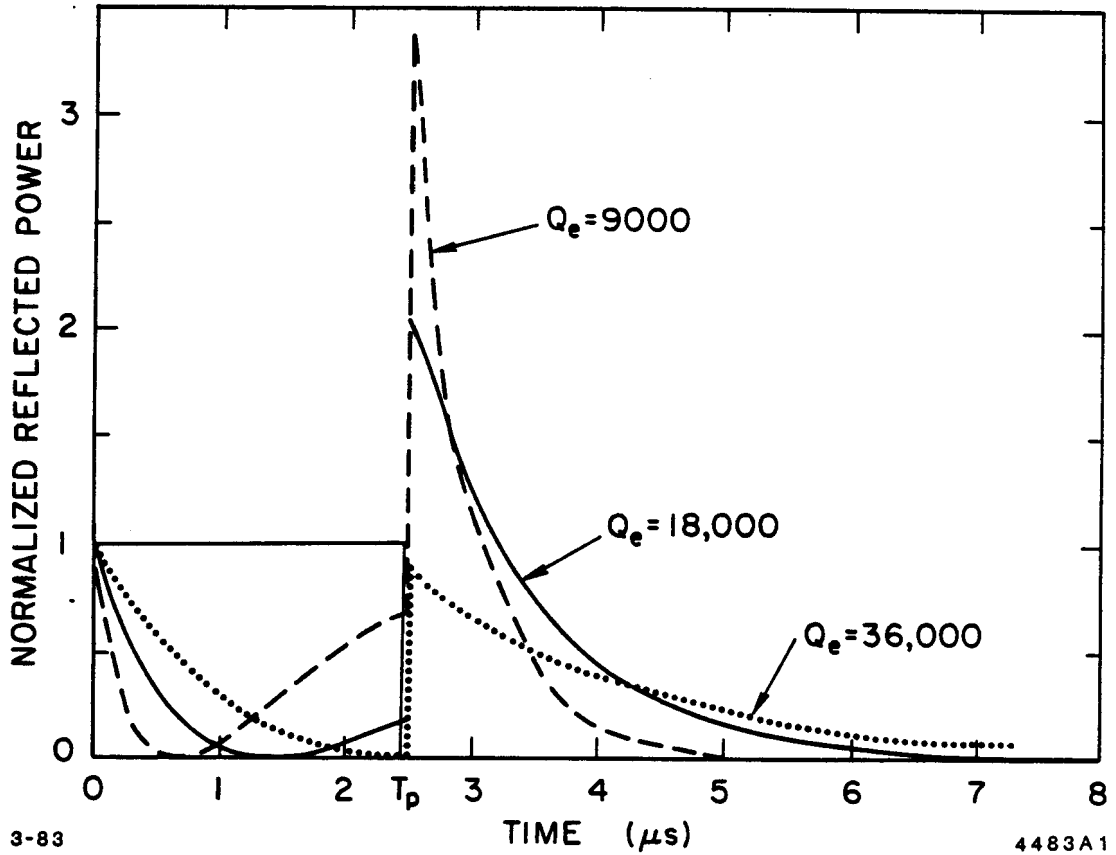
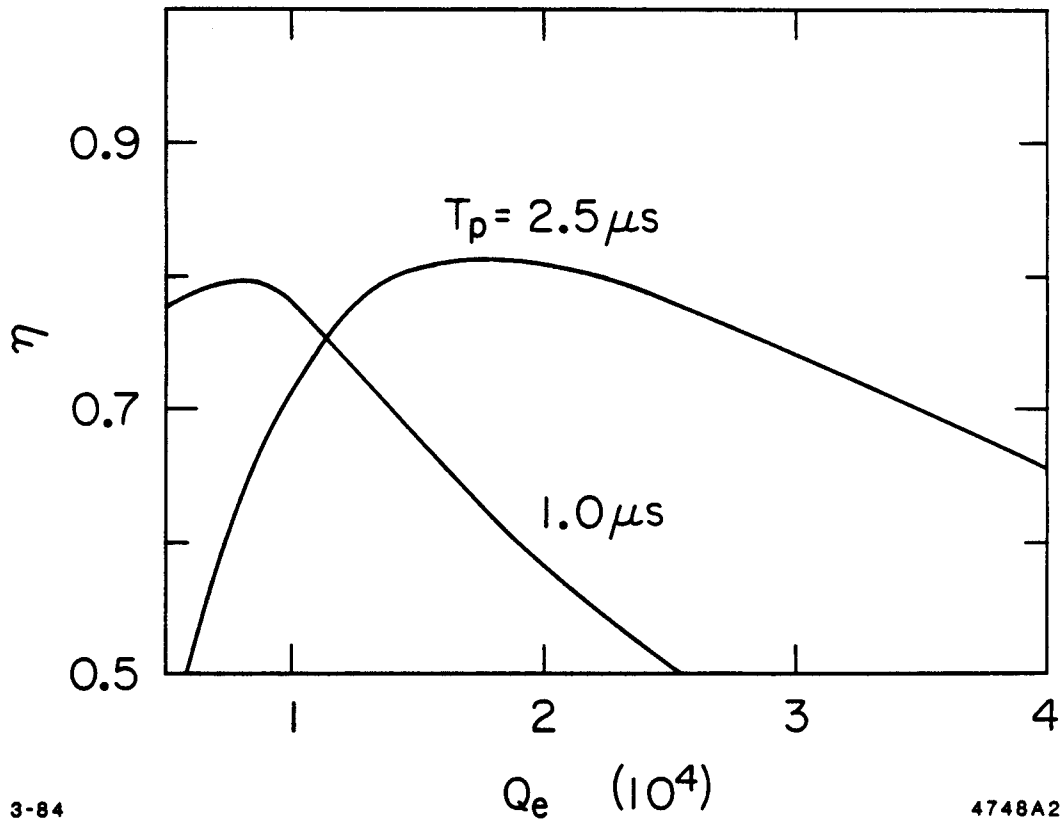


Fig. 1. Power reflected from the cavity as a function of time during and after the rf pulse. Three different Q_e are shown: $Q_e = 18,000$ gives the best transfer efficiency ($\eta \approx .80$; $f = 2856$ MHz).



3-84

4748A2

Fig. 2. Transfer efficiency of the pulse energy into the cavity as a function of Q_e . Two different pulse lengths are indicated here.

where k, k' are coefficients determined by computer programs such as LALA or SUPERFISH and, for a typical accelerator TM_{010} cavity, are of the order of $k \sim 75-80 \frac{MV}{m\sqrt{J}}$, $k' \sim 1400-1500 \frac{Q_e}{\sqrt{J}}$.

The actual determination of the peak energy stored in the cavity is done by using an average power meter, which, when properly gated, integrates the emitted power. The average power meter also sums the pulses reaching its sensor each second, so that the actual reading of the meter (once corrected for losses and calibration of couplers) must be divided by the repetition rate in order to obtain the energy stored at each pulse. Therefore

$$E_s = k \sqrt{\frac{P_e}{PRF}} \quad (5)$$

PRF being the pulse repetition frequency and P_e the average emitted power read on the meter and corrected for losses and coupling factors. Figure 3 illustrates the principle of integration of the emitted power.

3. Pulsed Power Measurements Apparatus

The experimental apparatus which is necessary to determine the fields in the cavity using Eq. (5) is in principle very simple: a calibrated coupler samples the emitted power; a PIN diode modulator, properly gated by a pulse generator, is used to allow only the emitted power to reach the power meter, which performs the integration. Figure 4 illustrates the scheme for the apparatus.

In practice the system used is considerably more complicated (Fig. 5), as several diagnostic tools are used to monitor the cavity behavior, in particular for the determination of the point at which the superconducting cavity is turning normal. The details of the system and its operation are contained in Ref. 6. Other diagnostics are done by monitoring the x-ray output, both correlated with the pulse (scintillator and phototube) and as average output (x-ray survey meter). During operation at 4.2 K we can observe the helium boiloff rate, in order to determine the field levels at which losses start to increase. A few resistor thermometers are used to check the cavity temperature at breakdown.

The cavities have fixed coupling with $Q_e = 16,000-22,000$ and are assembled at the end of a special transmission line with a transition which allows cryopumping into a copper rectangular waveguide rather than into the cavity (Fig. 6).

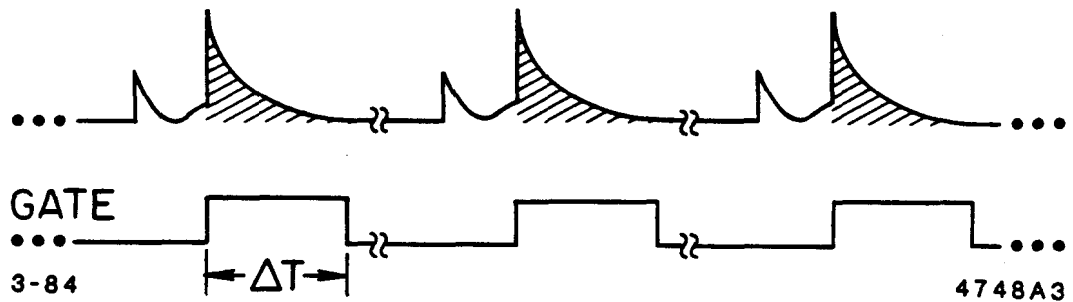
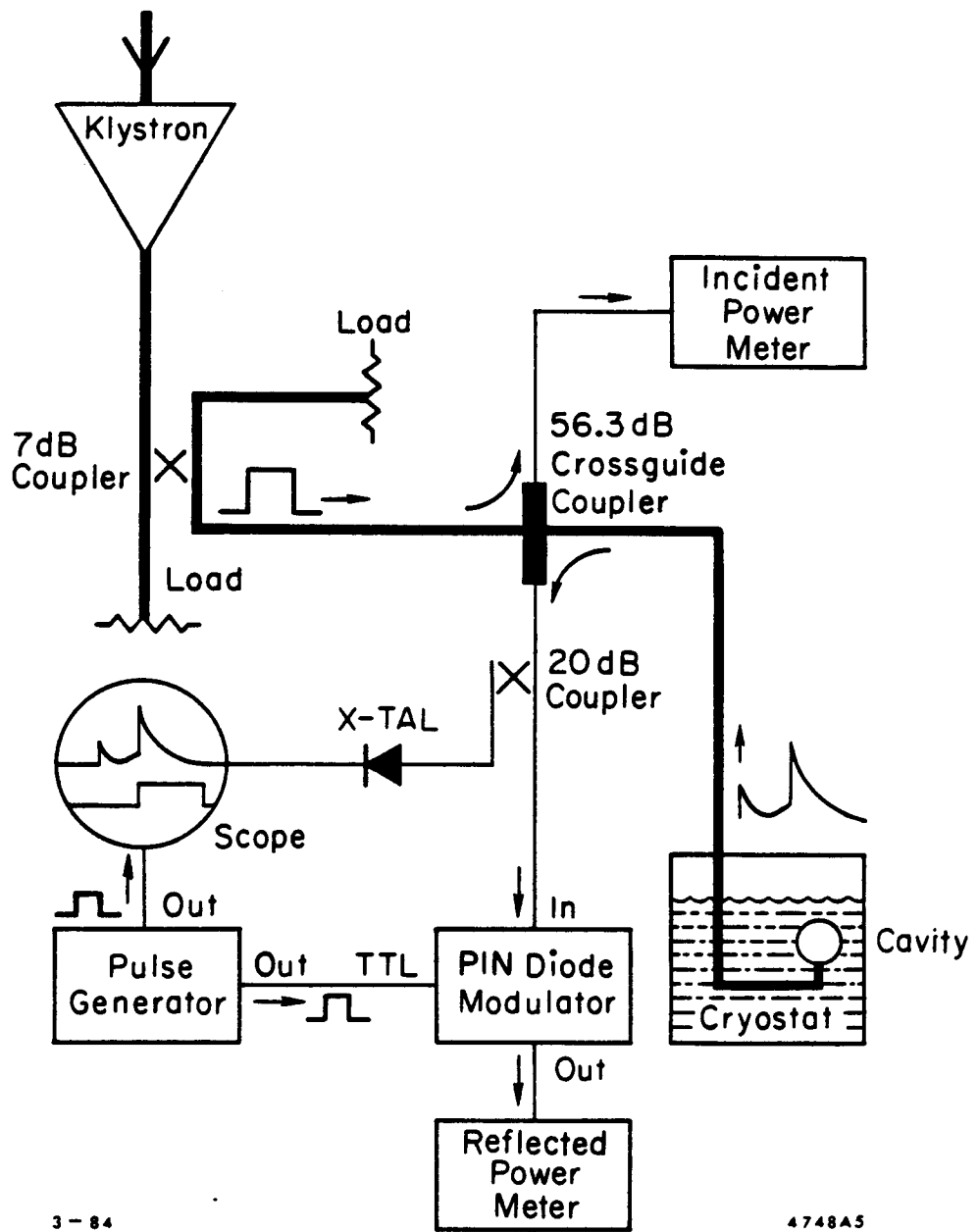


Fig. 3. The energy stored in the cavity is determined by integrating the emitted power curve (shaded area) using a gate which allows only that portion of the reflected power to reach the sensor.



3 - 84

4748A5

Fig. 4. Experimental setup necessary to perform the integration of the emitted power curve.

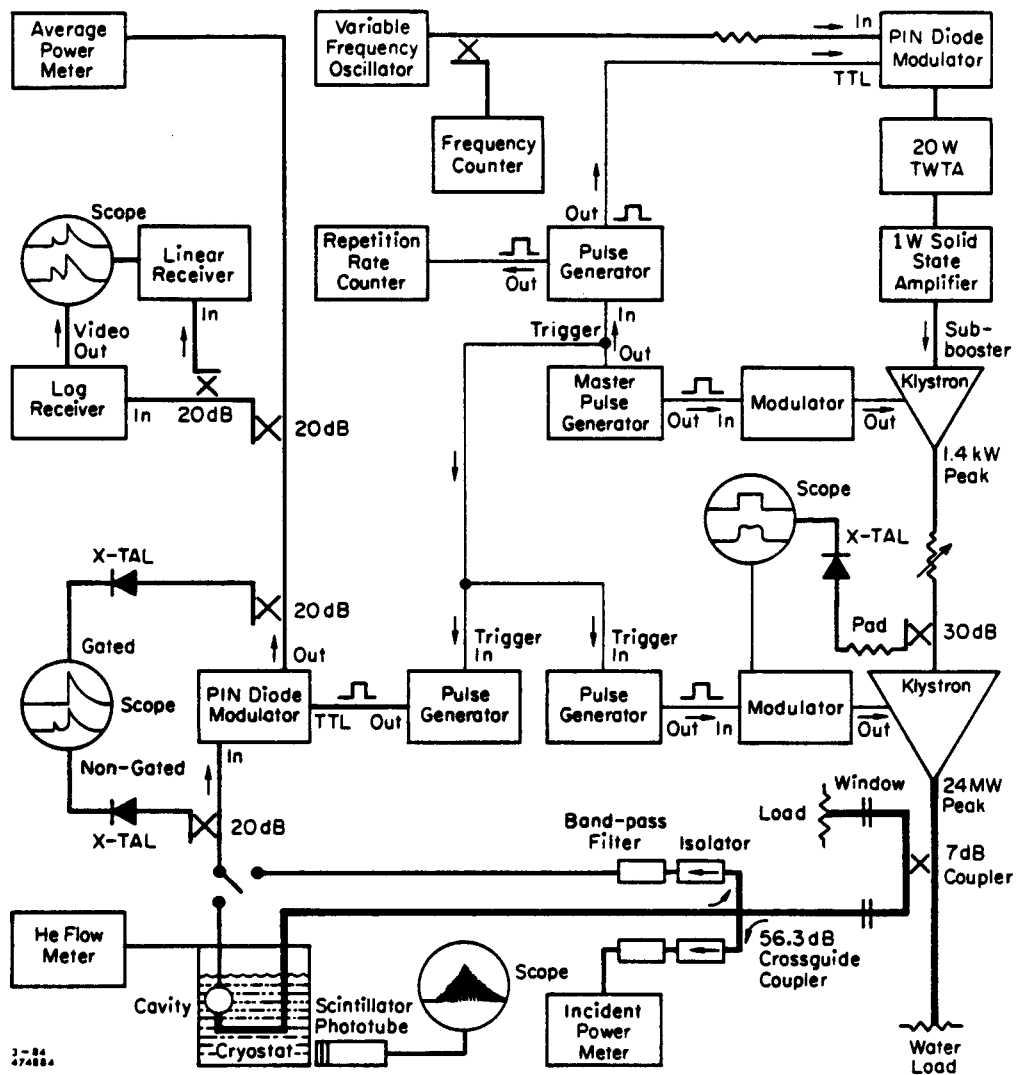


Fig. 5. Actual system used in the pulsed rf superconductivity tests, with the parts that allow variable pulse length operation and with the emitted power detection and diagnostic systems. The heavy lines indicate the high-power waveguide, the medium lines show the medium- and low-power rf cables and the light lines indicate the pulse control system.

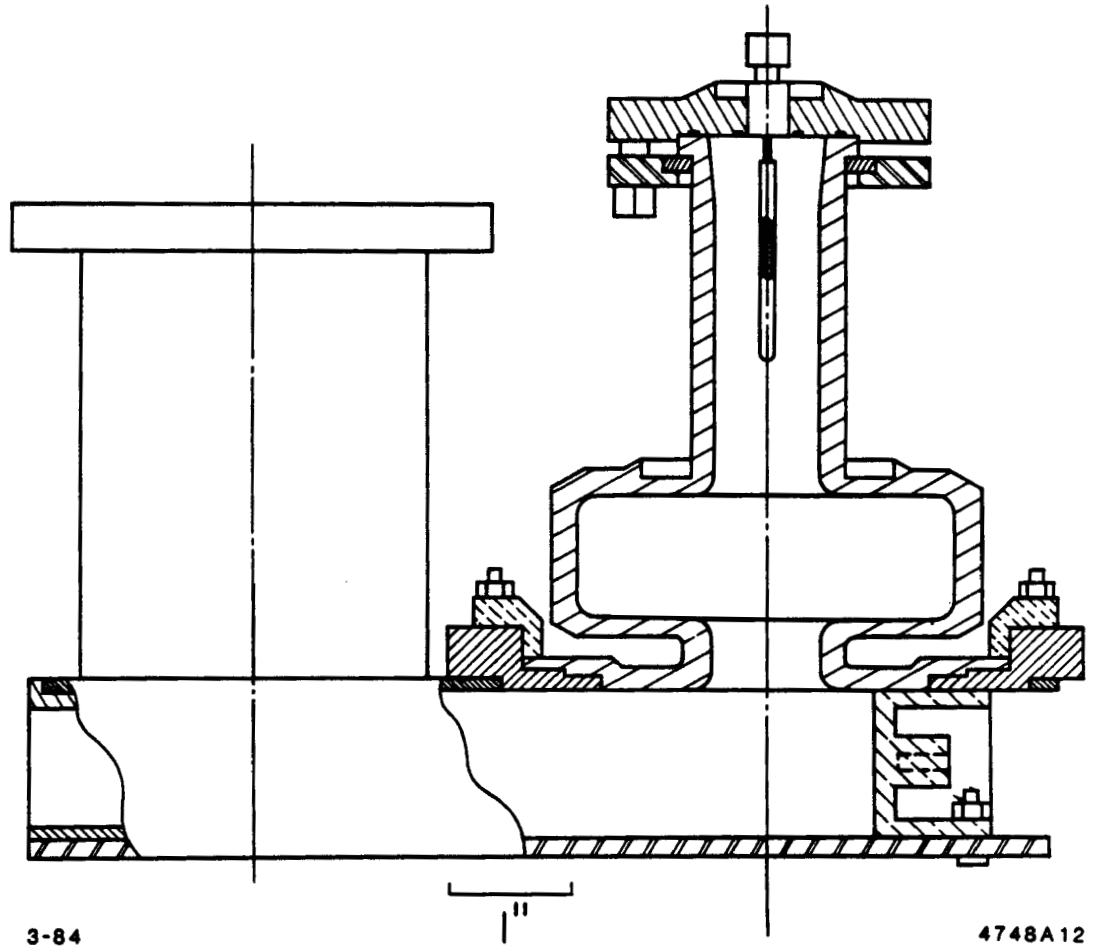


Fig. 6. Transmission line with fixed-coupling transition. The circular waveguide is connected to a rectangular-waveguide copper transition which prevents cryopumping into the cavity.

3.1 POWER CALIBRATION AND GATING

In the experimental method employed by us, two quantities must be accurately measured for the determination of the fields in the cavity: the first is the power attenuation through cables, isolators, filters and couplers from the cavity to the average power meter and the second is the location of the gate to the PIN diode modulator that allows only the emitted power to be sensed by the power meter.

The first quantity has been measured several times, almost always with an agreement at the 1% level in power, or less. This level is also the absolute power calibration rating of the power meters, so that the 1% level in power is taken to be the typical error in our calibration measurements. The attenuation calibrations have been performed using several different procedures, always in agreement among themselves at the 1% level. Attenuation measurements performed in cw and with pulses always agreed with the same accuracy quoted above.

The location of the PIN diode modulator gating pulse is determined by sampling the reflected power with a coupler and detecting it with a crystal rectifier immediately past the modulator itself, so that time delays through cables between the gating pulse and rf pulse are minimized. By repetitively setting, moving and resetting the gate at the end of the charging pulse, we always attained agreement at the 1% level. Our estimate of the upper limit for a possible systematic error in setting the gate is 3% or less; that is, if we would set the gate in the wrong position by ≤ 50 ns because of an error in the time delay between gate and rf pulse, then we would overestimate the emitted energy by no more than that amount. On the other hand, if the gate is delayed by a systematic given amount, then we would underestimate the emitted power by a larger percentage. This implies that, apart from grossly systematic errors in opening the gate too soon, our figures are in general lower limits to the actual fields.

3.2 EXPERIMENTAL DETERMINATION OF THE FIELDS AT BREAKDOWN

As a general tool for examining the peak field properties of the cavities tested and to determine at which peak field level the superconductivity is lost, we use the curves obtained by plotting the average emitted power versus the average incident power as read by the average power meters. The detailed shape of these curves (Figs. 7-10) vary from cavity to cavity, from repetition rate to repetition rate, from pulse length to pulse length. In principle these curves contain a lot of information

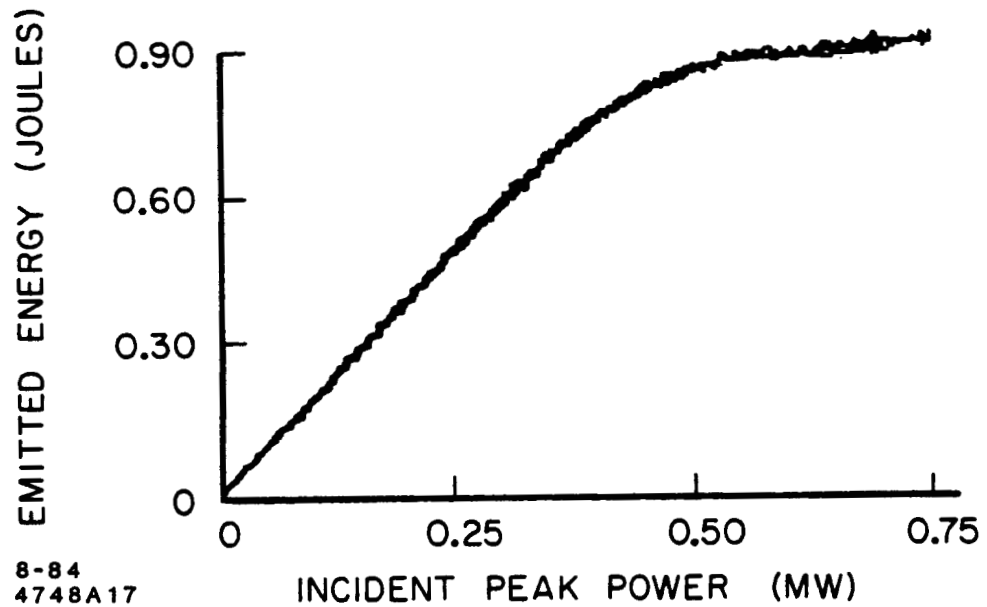


Fig. 7. Typical average emitted power versus average incident power curve obtained with the system of Fig. 5. This particular curve was obtained for cavity Leapfrog 2(LF2) at $T = 2^\circ\text{K}$, $T_p = 2.5 \mu\text{s}$, $PRF = 51$ pps.

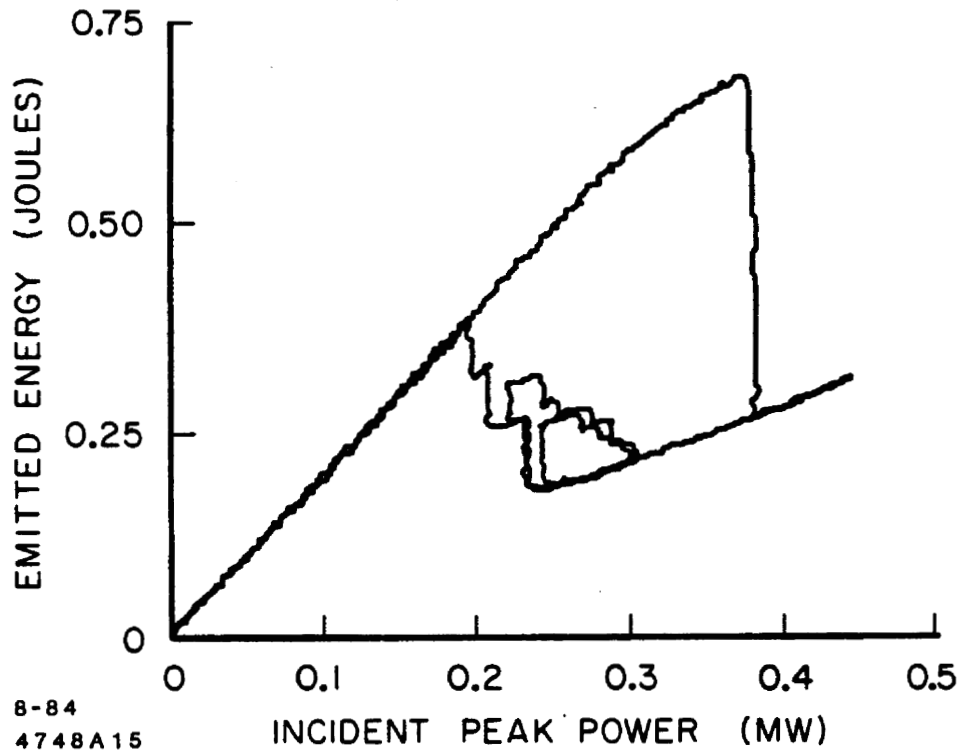


Fig. 8. P_e vs. P_i curve for cavity LF2, $T = 4.2^\circ\text{K}$, $T_p = 2.5 \mu\text{s}$, $PRF = 82$ pps. In this case hysteric loops are observed, connected with *He* film boiling at the cavity's outer surface.

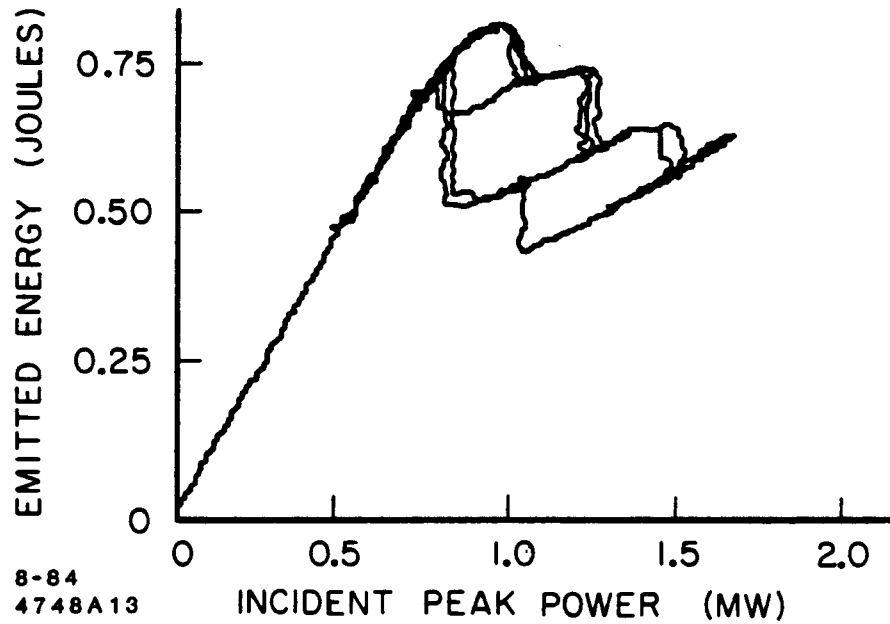


Fig. 9. Other hysteretic loops observed in the P_e vs. P_i curve for the SLAC cavity; $T = 4.2^\circ\text{K}$, $T_p = 1.25 \mu\text{s}$, $PRF = 59$ pps. Each loop is probably induced by *He* film boiling at various regions of the external surface.

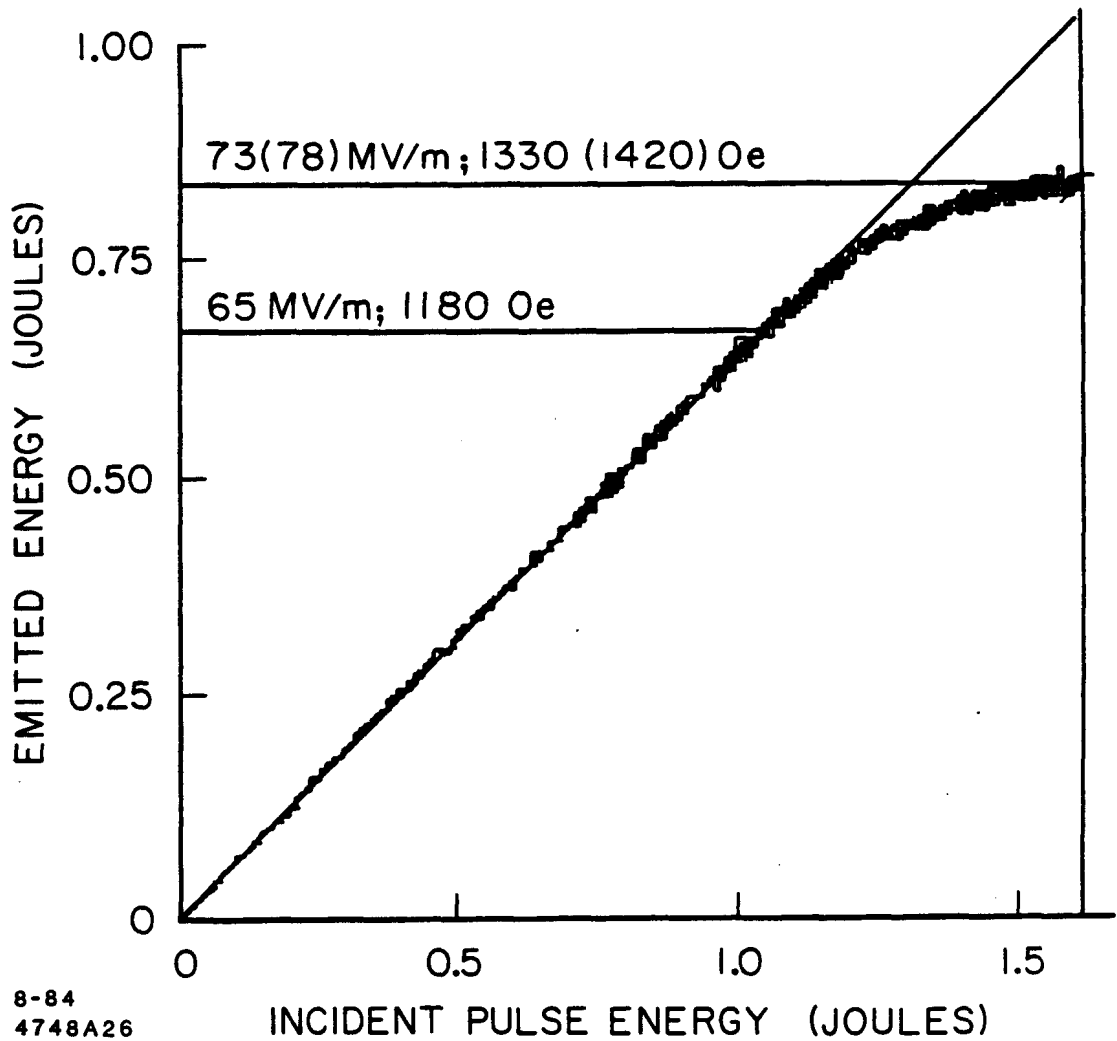


Fig. 10. The maximum peak fields in the cavity are determined by determining the point in the P_e vs. P_i curve which shows a deviation from a straight line passing through the origin and following the initial linear part of the curve itself. This curve was obtained for cavity LF5, $T = 1.4^\circ\text{K}$, $PRF = 51$ pps, $T_p = 1 \mu\text{s}$.

about the losses in the cavity, whether caused by rf, electron loading and heating, about the heat transfer to the bath and so on. In practice, it might be very difficult, if not impossible, to retrieve all of the information, especially by the use of these curves alone.

When the losses in the cavity are negligible or if they are constant with field level the emitted energy is proportional to the incident power, so that the P_e vs. P_i curves are straight lines. The slope of the straight lines depends on the exact value of the external Q_e , since $P_e = \eta P_i$, where η is the energy transfer efficiency, which is a constant dependent on Q_e [see Ref. 6, Eq. (1)]. But as the losses in the cavity increase, η is no longer constant and the function $P_e = P_e(P_i)$ assumes a complex shape. The point at which $P_e(P_i)$ departs from the linear behavior is taken as the maximum level for which useful fields can be stored (although for a short time) without additional losses. The position of such a point in the $P_e(P_i)$ curve has been checked carefully against other symptoms normally used to identify the increase of losses in a cavity. These methods involve the observation of the increase in helium boiloff rate at 4.2°K and of the power decay curve. This latter method is not extremely sensitive because the cavity is strongly coupled, so that changes in the power decay rate can only be observed if Q_0 has decreased by a few orders of magnitude from the low-loss value.

The determination of the increase of losses using the helium boiloff rate at 4.2°K is somewhat more sensitive, but it is repetition rate dependent. As discussed in Ref. 6, the average losses in the cavity during a pulse can be expressed as

$$\frac{1}{Q_0} \simeq \frac{1}{\eta} \frac{5.5}{\omega T_p} \frac{P_d}{P_i T_p PRF} \quad (6)$$

where η is the pulse energy transfer efficiency, P_i is the peak incident power of the rf pulse, T_p is the pulse length, PRF is the pulse repetition frequency and P_d is the average power dissipated into the bath. The largest Q_0 below which the increase in boiloff can be detected using a laminar flow element manometer with a sensitivity of $P_d \simeq 15$ mW is given, for our operating frequency of 2856 MHz and a pulse length of 2.5 μ s, by

$$Q_{0,thr} \simeq 4.2 \times P_i \times PRF \quad (7)$$

For typical operating parameters, the threshold \bar{Q}_0 has been determined to be close to the Q_0 measured by low-power, cw methods. The portion of the charging and discharging pulse which actually contributes to the losses is, at that threshold power level, very short, but the Q_0 during that time must drop by a few orders of magnitude in order to give an observable boiloff rate increase.

Among these three major methods used to pinpoint the field level at which the full superconducting state is lost (decay curve, the boiloff, $P_e(P_i)$ curves), the one that makes use of the P_e vs. P_i curve seems to be the most sensitive: in all the measurements the deviation from linearity of the P_e vs. P_i curve always preceded the increase in boiloff and the observable change in the power discharge rate. Therefore, this method has been used more than any other in order to determine the breakdown field.

4. Test Results

4.1 RESULTS OF THE TESTS ON Nb CAVITIES

These results have been thoroughly discussed in Ref. 6, so that here we will only summarize the main features of the experimental results.

Six niobium cavities of two different shapes were tested, after being fitted with a fixed-coupling iris and fired at 1950°C (Figs. 11-12). The cavities were tested at cw first and a variety of performances were observed: some of them could reach relatively high fields (considering that they were tested without any particularly sophisticated surface preparation) while others had very poor performance both in Q_0 and maximum field at breakdown, probably limited by bad spots and spattered Nb droplets (Table 1).

- Under pulsed operation all the cavities show similar properties, as far as the maximum obtainable field is concerned, totally unrelated to the cw behavior.
- Pulses of 1 μ s length usually enable us to reach higher fields than 2.5 μ s pulses.

Table 1
Low-power, long-pulse test results on Nb cavities

Cavity	Temp (K)	$Q_{0\max}$	$E_{s\max}$ (MV/m)	$Q_0 (E_{\max})$	Remark
SLAC	4.2	9.6 E7	5.8	9.0 E7	after firing
SLAC	1.3	2.3 E9	22.3	1.4 E9	after firing
SLAC	4.2	8.9 E7	7.2	8.6 E7	after In strip
SLAC	1.3	1.1 E9	13.4	1.0 E9	after In strip (present)
LF1	4.2	9.9 E7	17.3	7.2 E7	
LF1	1.3	5.4 E8	24.9	4.5 E8	$X = 150$ mR/hr
LF2	4.2	7.6 E7	4.2	5.1 E7	
LF2	1.3	6.0 E8	4.4	1.7 E8	
LF3	4.2	7.7 E7	8.3	5.8 E7	
LF3	1.3	3.0 E8	7.6	1.9 E8	
LF4	4.2	9.9 E7	14.8	7.0 E7	
LF4	1.3	8.9 E8	23.2	2.3 E8	$X = 150$ mR/hr
LF5	4.2	9.3 E7	9.2	7.7 E7	
LF5	1.3	1.1 E9	10.3	9.8 E8	

The results of the high-power tests can be summarized as follows (Table 2):

Table 2
Summary of peak surface fields reached before degradation of Q_0

Cavity	4.2°K 2.5 μ s			4.2°K 1 μ s			1.4°K 1 μ s		
	PRF (pps)	E_s (MV/m)	H_s (Oe)	PRF (pps)	E_s (MV/m)	H_s (Oe)	PRF (pps)	E_s (MV/m)	H_s (Oe)
SLAC	82	59	1120	40	68.4	1300	33	67	1280
LF1	82	56	1020	57	60.6	1100	33	58	1060
LF2	82	58	1060	50	58	1060	51	58	1060
									(2.5 μ s)
LF5	82	60	1090	51	67	1220	33	65	1180

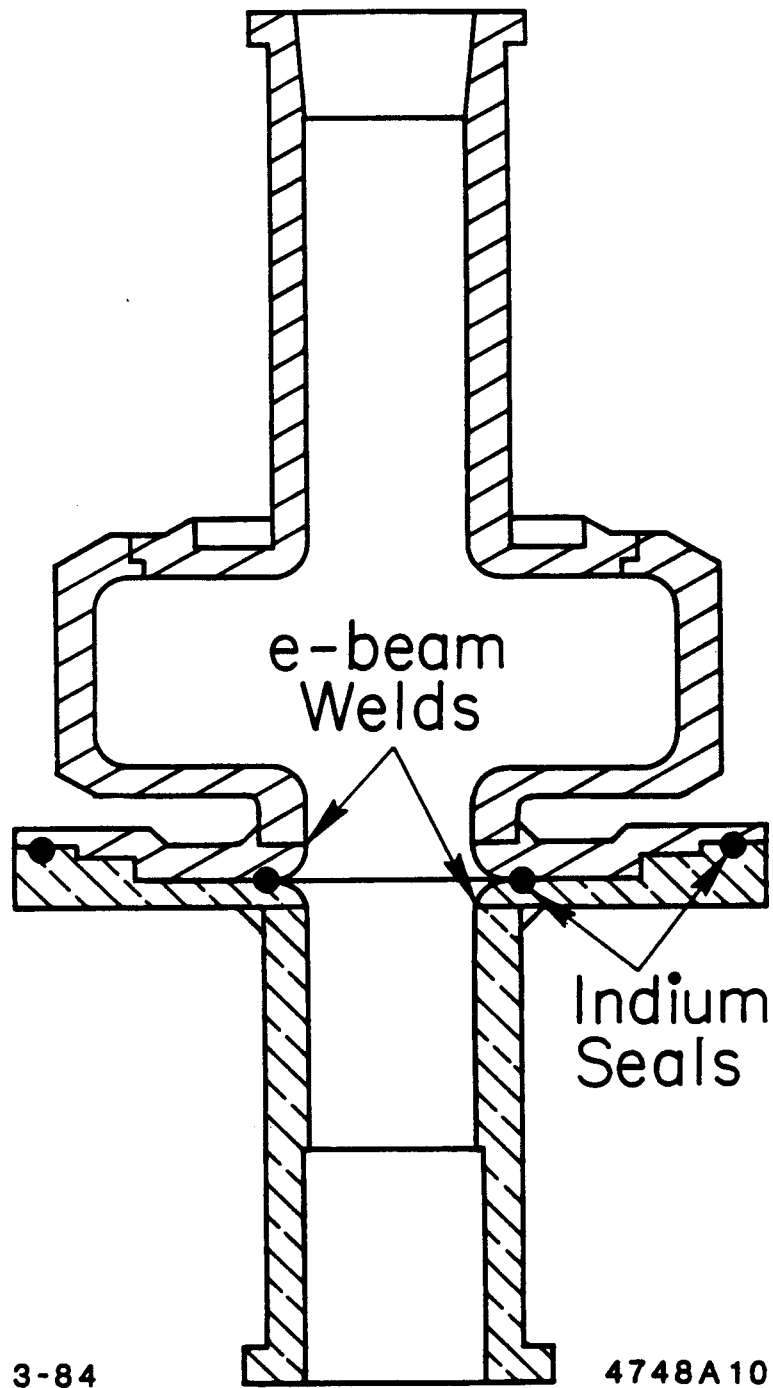


Fig. 11. Cross section of the modified SLAC TM_{010} Nb cavity. This cavity was originally built in 1971 with two cutoff tubes. One of them was recently removed to allow for fixed coupling, pulsed operation. A double-flange assembly permits long-pulse, low-power tests.

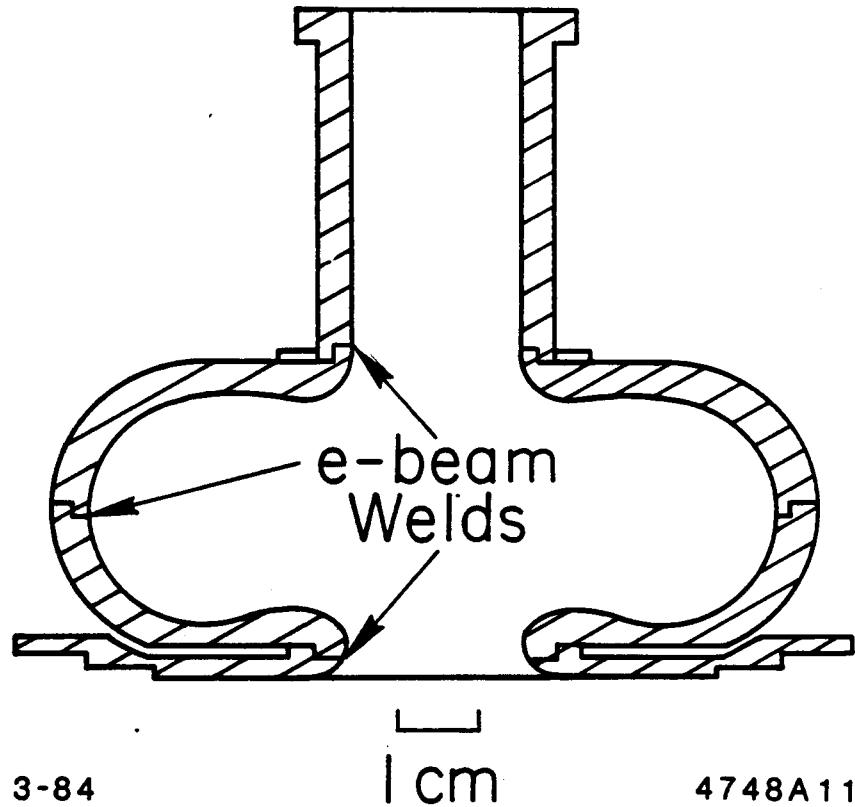


Fig. 12. Cross section of one of the LEAPFROG (LF) Nb cavities. Several coined halves were recently assembled for the purpose of testing them in the pulsed mode and later coat them with Nb_3Sn .

- There is **no** detectable difference between the maximum attainable field at 4.2°K and at lower temperatures, down to 1.4°K (Figs 13-14).
- Strong erratic x-ray emission is initially observed during the turn-on stages of the tests on each cavity, emission that quickly disappears (rf processing).
- A weaker x-ray emission, correlated in time with the maximum fields in the cavity, is always present and does not seem to decrease either with time, or with rf or helium processing.

This latter radiation, which starts to appear at peak surface electric field levels of ~ 35 MV/m, is somewhat correlated with the increase in losses, but cavities with different x-ray emission intensities have approximately the same breakdown field.

In summary, it seems possible at the moment to operate *Nb* cavities at peak surface electric field levels of ~ 60 MV/m with pulse lengths of $2.5 \mu\text{s}$ and at a temperature of 4.2°K, without any particularly difficult preparation of the cavities themselves. This proves that, over short times, the superconductor is not defect-limited.

4.2 RESULTS OF THE TESTS ON LEAD-PLATED COPPER CAVITIES

As a part of the program to test the technical rf superconductors under pulsed conditions, we have begun testing lead-plated copper cavities built at SLAC and plated in collaboration with John Dick of Caltech. A more detailed paper on the subject is now in preparation.⁷

So far tests have been performed on two cavities. They are built out of OFHC copper, with a design similar to one of the *Nb* cavities tested previously (Fig. 15). Unlike for the *Nb* cavities, the coupling iris does not have a deep external groove for cooling. The cavities are built out of two halves, joined at the equatorial plane by a *Cu Au*, hydrogen furnace brazed joint: this joint seems to be adequate for the purpose and the technique is well under control at SLAC. The two cavities have slightly different external *Q* (16,000 and 22,000), so that some of the details in the behavior are expected to be somewhat different.

As a first test it was decided to plate the cavities without performing on them the more complicated process of chemical polishing, which was successfully developed at Caltech. The coating thickness is different for the two cavities and was computed to be approximately 15 and 6 μm , respectively. The final surface showed the underlying

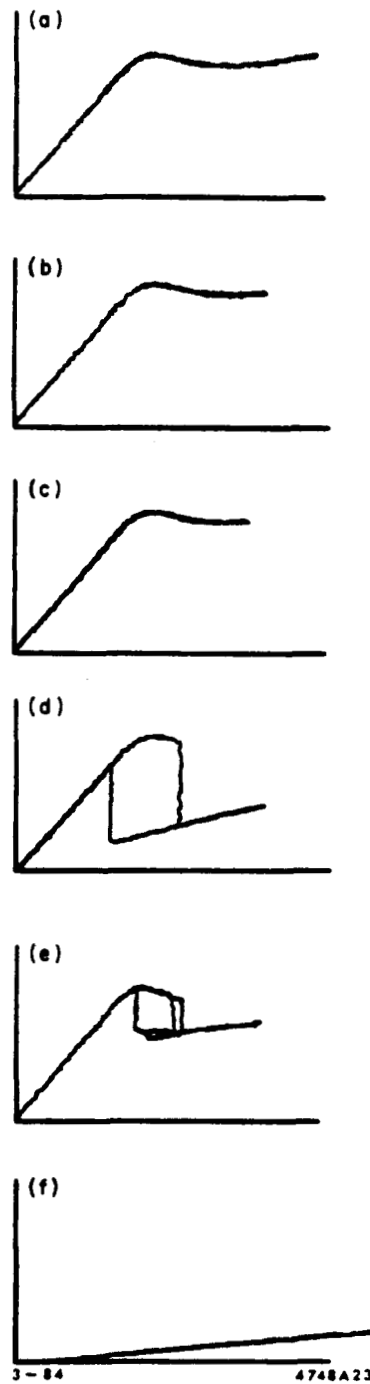


Fig. 13. Temperature variation of the P_e vs. P_i curves for cavity LF1, $T_p = 2.5 \mu s$, $PRF = 51$ pps. The temperatures are: a) $1.4^\circ K$, b) $1.7^\circ K$, c) $2.0^\circ K$, d) $2.2^\circ K$, and e) $3^\circ K$. For comparison the cavity was tested normal at $77^\circ K$ (f).

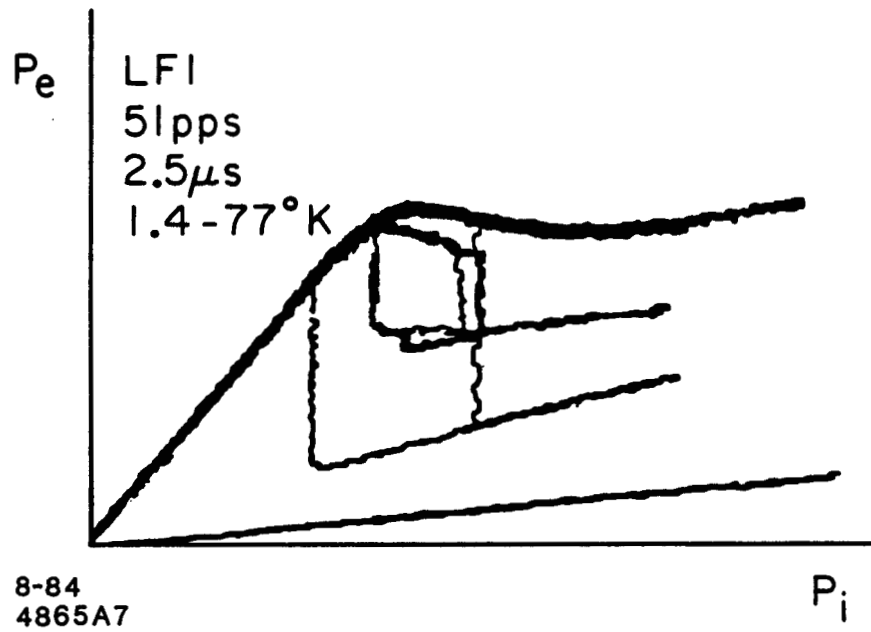


Fig. 14. Overlap of all the curves of Fig. 13. All of the curves coincide at least up to the inflection point, indicating a negligible temperature dependence of the fields that can be reached without losses.

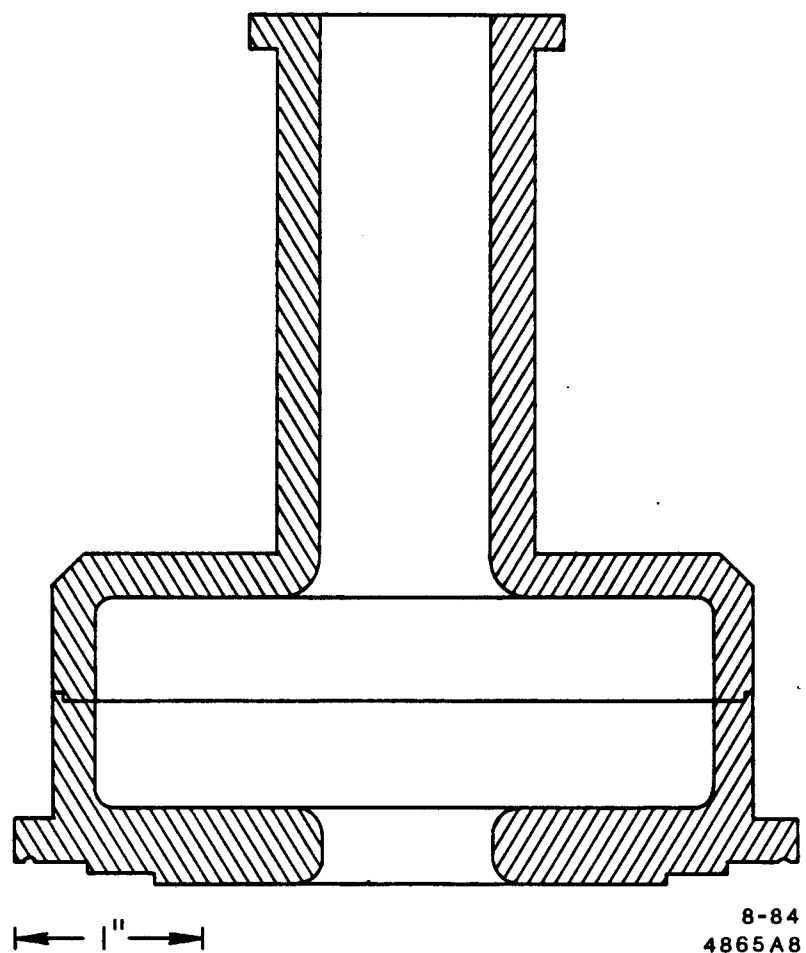


Fig. 15. Cross section of the copper cavities prepared for lead or tin plating. The design is similar to that of the cavity in Fig. 11 but there is no cooling groove close to the coupling iris.

crystal structure of the copper and, not having been polished, did not have the reflectivity of other lead surfaces treated in that way.

The lead-plated cavities were tested in the same way niobium cavities were tested, with various repetition rates, pulse lengths and at various temperatures.

The most striking difference between the *Nb* cavities tests and the lead plated ones is that while for the *Nb* the P_e vs. P_i curves inflected at the same point, irrespective of temperature, the lead plated cavities show a very clear temperature dependence of the inflection point (Fig. 16-17). For cavity "Pb2" this deviation from linearity is sharper than for "Pb1". This fact could be ascribed both to the larger $Q_e = 22,000$ and/or to the thinner coating of lead ($6 \mu\text{m}$).

The second most important feature is that when operated with $1 \mu\text{s}$ pulse and low repetition rate, the field determined by our standard method seems to exceed, at any temperature, the theoretical value for the superheated field by about 100-150 *Oe* (Table 3 and Fig. 18). For high repetition rates (360 pps) and $2.5 \mu\text{s}$ pulses the field at 4.2°K seems to coincide with the superheated one and is slightly lower for lower temperatures (Fig. 19). We have checked for any possible source of error involved in the measurements but all the checks seem to indicate that the data are correct. At the moment the only plausible explanation seems to be that the critical field has to be exceeded by a fixed amount at any temperature, in order to have enough dissipation, over the fraction of the microsecond pulse during which the critical field is exceeded, to show up on the \dot{P}_e vs. \dot{P}_i curves. The data at temperatures higher than 4.2°K were obtained by lowering the liquid helium level below the cavity, but touching the copper waveguide at the bottom of the transmission line (Fig. 6) and by pressurizing the vapor. For this reason the curves at higher temperature are qualitatively different, but thermometry checks indicate that we can still pinpoint the field level at which losses increase.

A strange phenomenon seems to occur at field levels of $\sim 600\text{-}700 \text{ Oe}$ (30-35 MV/m peak surface electric field) which was not observed in the *Nb* cavities: correlated with the onset of x-rays and, at 4.2°K , with a slight increase in boiloff, we observe a slight change in slope of the \dot{P}_e vs. \dot{P}_i curve, which is approximately a straight line. This change of slope occurs always at the same field level irrespective of temperature and cannot, therefore, be ascribed to rf losses induced

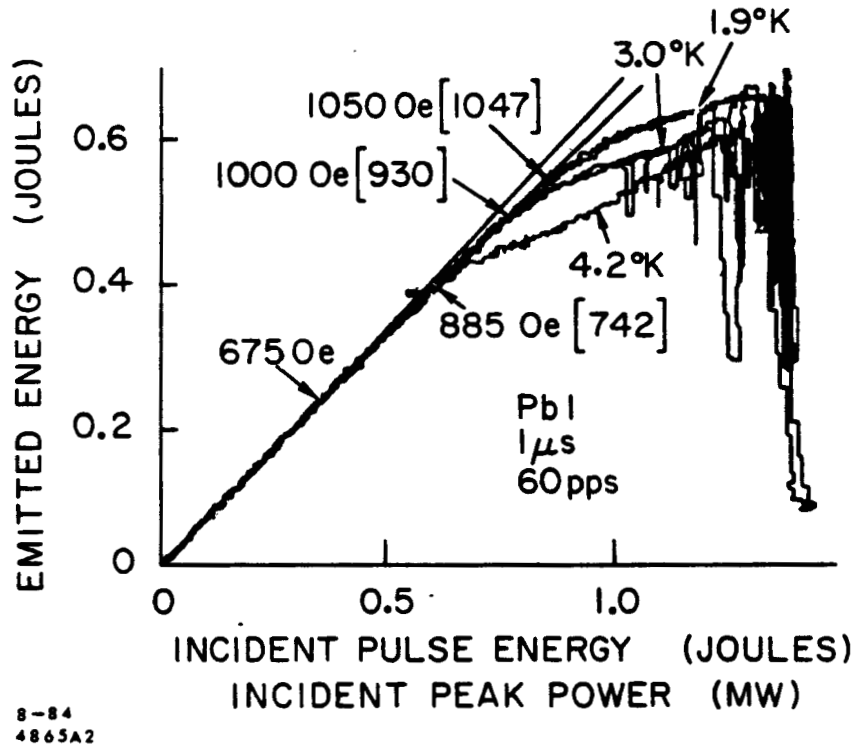


Fig. 16. Emitted energy curves for the lead cavity Pb1, for the parameters indicated. The various curves were taken at different temperatures. The arrows point to the magnetic field level for which deviation from linearity starts. The square brackets contain the theoretical super-heated field for the corresponding temperature. The arrow at 675 Oe points the level at which a small change in slope occurs, which might be due to field emission at the coupling. The sharp energy drops toward the upper end of the curves are due to sudden detunings of the cavity induced by strong field emission bursts. These bursts tend to disappear in a matter of minutes.

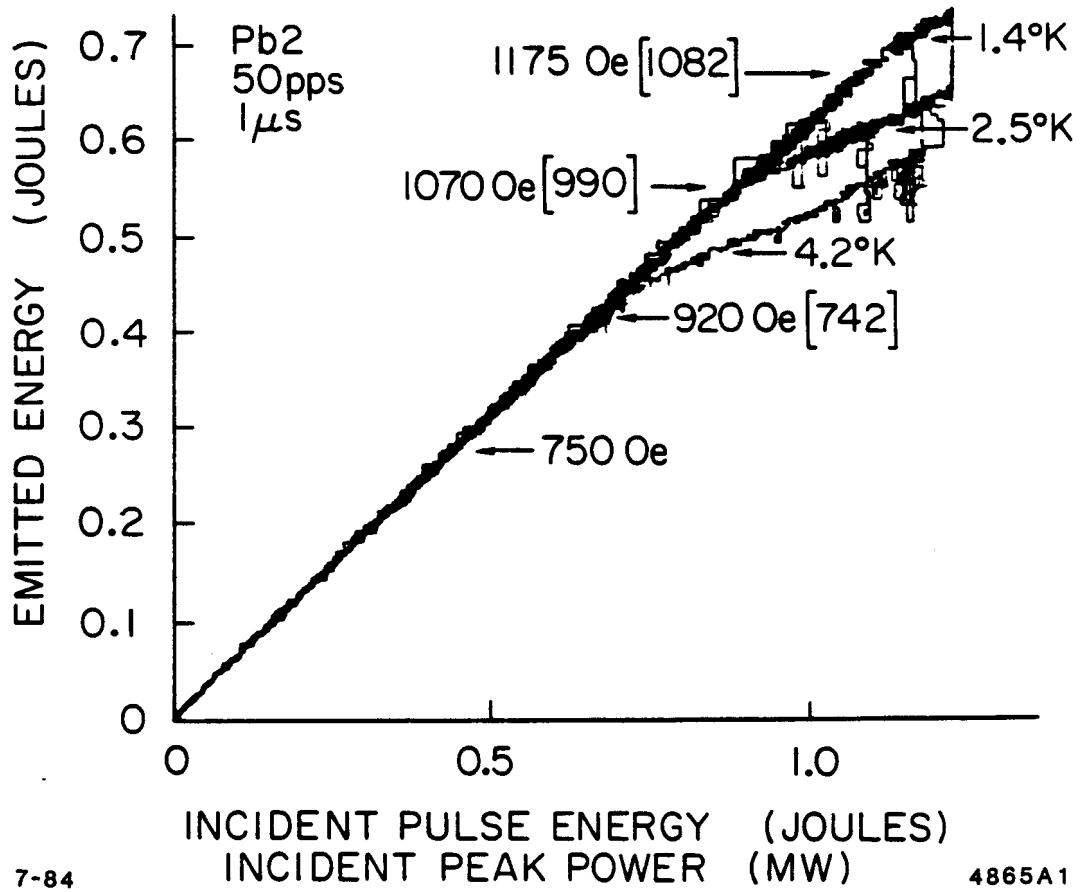


Fig. 17. Curves similar to the ones in Fig. 16 for cavity Pb2.

Table 3
Temperature dependence of breakdown field in Pb
(cavity Pb1, 1 μ s pulse length, $PRF = 60$ pps)

$T(K)$	$H_{exp}(Oe)$	$H_{sh}(Oe)$ (theory)
1.9	1050	1047
3.0	1000	930
4.2	885	742
4.7	771	646
4.9	708	604
5.2	623	538
5.4	551	492
6.0	491	344
6.5	311	208
7.0	214	62
7.1	137	31

by exceeding a critical field. A possible reason could be a slight change of Q_e due to field emission at the iris, which is effectively restricted by the field-emitted current. This hypothesis seems to be corroborated by the fact that at high field levels, when total field-emission breakdown is observed, the observation of both reflected and transmitted power curves show that total detuning-loading occurs in the two curves in an almost totally uncorrelated way, with reflected power shortings occurring more often than for the transmitted power and at a rate of several times higher. This fact implies that energy can be stored in the cavity at higher field levels than previously thought, and that perhaps appropriate redesign of the iris might allow us to decrease the field-emission problem, perhaps even in the Nb cavities.

In summary, preliminary tests on lead-plated copper cavities indicate that at 4.2°K, 360 pps and 2.5 μ s pulse length the superheated critical field of lead can be attained without losses and without any preparation of the cavities. For shorter pulse lengths, fields as high as 900 Oe can be reached without appreciable average losses at the same temperature.

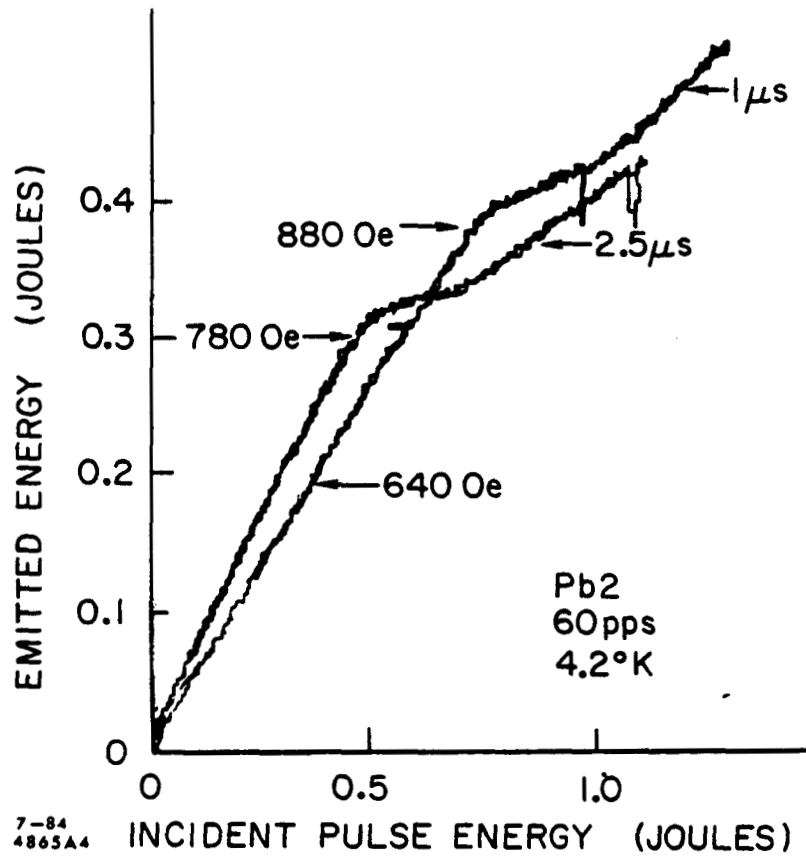


Fig. 18. Comparison between the emitted energy curves obtained with 1 μ s and 2.5 μ s pulse length for the cavity Pb2. The different field levels reached in the two cases before the onset of losses has not been explained yet. Occasional energy drops due to field emission can be seen throughout the curves.

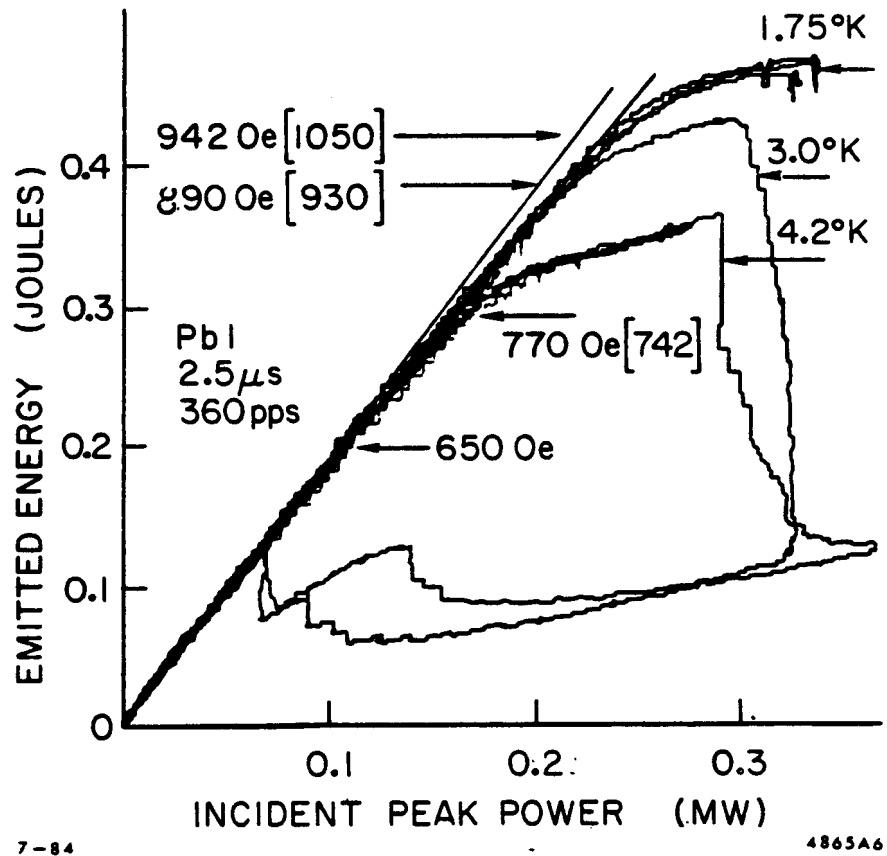


Fig. 19. Emitted energy curves obtained for cavity Pb1 in the hardest operating mode possible with out system, 360 pps repetition rate and 2.5 μs pulse length. The hysteretic loops are seen at these field levels in copper cavities only for these extreme parameters.

4.3 TESTS OF Nb_3Sn AND Sn

Tests are planned for Nb_3Sn cavities. Niobium cavities, built at SLAC, are being coated by tin evaporation at the University of Wuppertal by the group led by Professor H. Piel (Dr. G. Arnolds-Mayer, M. Peiniger). A first preliminary test on a cavity which, from the cw tests, showed patches of bare Nb and of excess tin, gave inconclusive results, except for the fact that its behavior was definitely not worse than that of Nb at 4.2°K. Other cavities are being readied and they will soon be tested.

The observed fields in Pb which in some cases seem to exceed even the superheated field, has convinced us that we should test a TM_{010} tin plated cavity: in this case the temperature dependence of the critical field can be more accurately followed than in the case of superconductors with critical temperatures above 4.2°K and, as the ratio of the superheated to thermodynamical critical fields is even higher than for Pb, we should answer some of the questions which have risen from the recent measurements on Pb.

Finally we should mention that a TE_{011} copper cavity which can be lead or tin plated is being readied. If the results of the tests on it will be of interest in determining peak rf field properties in superconductors without interference from field-emitted electrons and x-rays, then a similar Nb and Nb_3Sn cavity will be prepared.

5. Applications of Pulsed rf Superconductivity

While cw operation of superconducting accelerator structures requires improvement factors of about 10^6 in order to be of practical use, in the pulsed mode an improvement factor of $\sim 10^3$ can lead to applications competitive with room temperature operated systems. Among these applications we mention pulsed linear electron accelerators⁹ and traveling-wave, energy storage lossless delay lines for peak power multiplication.¹⁰

For a traveling wave section of a given length, pulsed rf superconductivity reduces the section losses so that the same accelerating voltage can be obtained with typical input power levels smaller by a factor of 1.7 with respect to room temperature structures. This type of operation lessens the requirements on both average

and peak power. Additional peak power reduction is attained because higher group velocities are possible. This effect is equivalent to having pulse compression without external energy storage. This type of scheme is being considered as a possible design for the CEBAF accelerator to be built by the Southeastern Universities Research Association.

6. Conclusions

The testing of superconducting cavities at SLAC using short pulses has established that higher peak fields can be reached without appreciable losses in some cases up to the theoretical field limits. The work will be extended to study the pulsed behavior in several superconductors and for other cavity geometries and modes. Theoretical work is in progress to try to explain the pulsed measurement features from first principles. In addition, the possibility of applying the method to actual practical systems for accelerators is being considered.

Acknowledgements

The authors would like to thank Perry Wilson for several stimulating discussions. H. Deruyter and J. Weaver were instrumental in the realization of parts of the project. Z. Zamzow was responsible for the smooth operation of the experiment.

References

1. J. B. Stimmel, Ph.D. Dissertation, Cornell University (1978).
2. T. Yogi, Ph.D. Dissertation, Caltech (1977).
3. T. Yogi, G. J. Dick, and J. E. Mercereau, Phys. Rev. Lett. **39**, No. 13, 826-829 (1977).
4. I. E. Campisi, Z. D. Farkas, H. Deruyter and H. A. Hoag, IEEE Trans. Nucl. Sci., NS-30, No. 4, 3366-3368 (1983).
5. Z. D. Farkas, SLAC/AP-15 (1984).
6. I. E. Campisi and Z. D. Farkas, SLAC/AP-16 (1984).
7. I. E. Campisi, G. J. Dick, and Z. D. Farkas, in preparation.

8. G. J. Dick, J. R. Delayen and M. C. Yen, **IEEE Trans. Nucl. Sci., NS-24, 1130 (1977).**
9. Z. D. Farkas and S. J. St. Lorant, **IEEE Trans. Mag., MAG-19, 1338 (1983).**
10. Z. D. Farkas, **SLAC/AP-17 (1984).**

